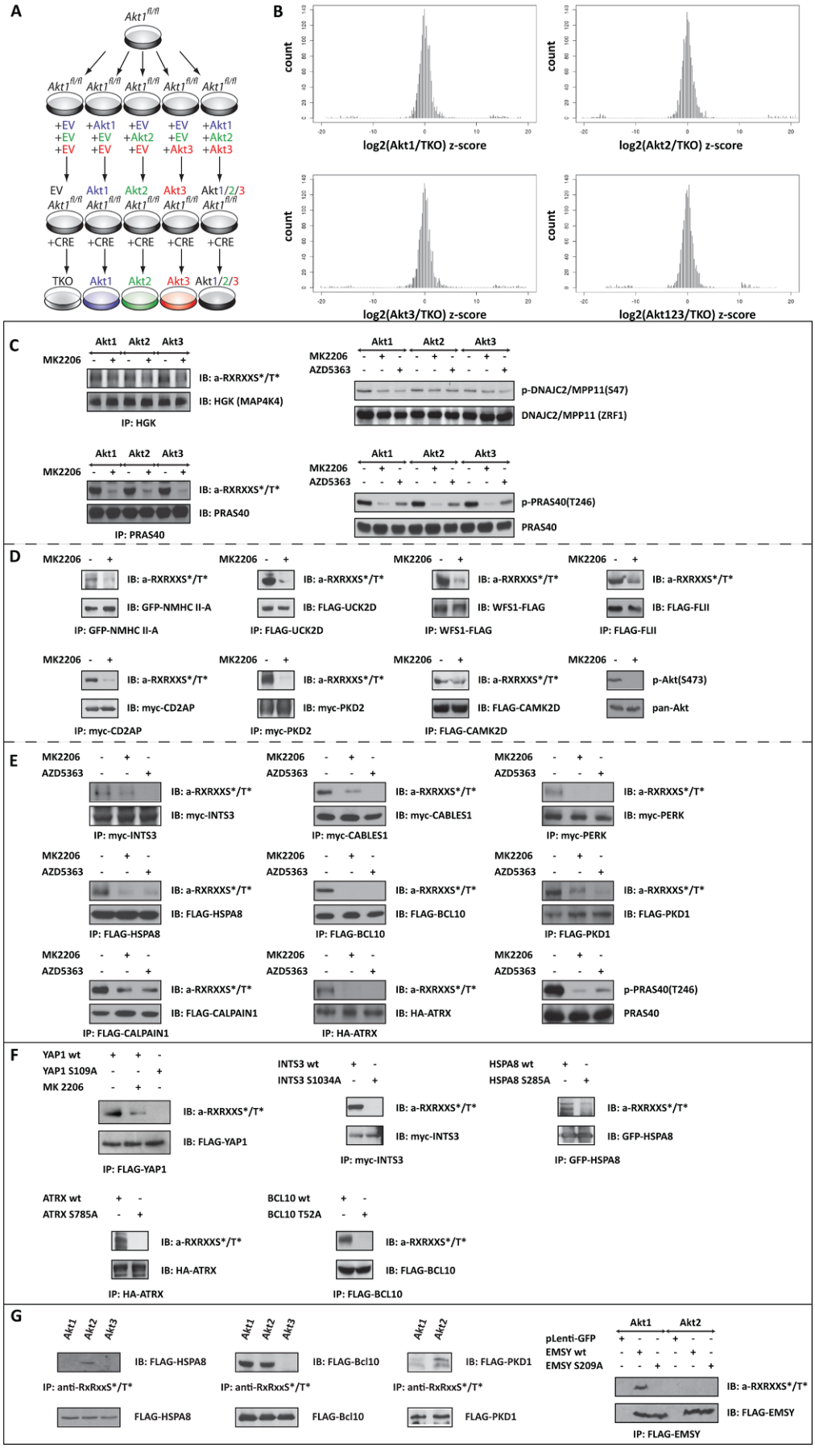
A
Akt1fl/fl
+EV
+Akt1
+Akt2
+Akt3
+CRE
EV
Akt1
Akt2
Akt3
Akt1/2/3
TKO
B
count
log2(Akt1/TKO) z-score
log2(Akt2/TKO) z-score
log2(Akt3/TKO) z-score
log2(Akt123/TKO) z-score
C
MK2206
AZD5363
IB: a-RXRXXS*/T*
IB: HGK (MAP4K4)
IP: HGK
IB: PRAS40
IP: PRAS40
p-DNAJC2/MPP11(S47)
DNAJC2/MPP11 (ZRF1)
p-PRAS40(T246)
PRAS40
D
IB: GFP-NMHC II-A
IP: GFP-NMHC II-A
IB: FLAG-UCK2D
IP: FLAG-UCK2D
IB: WFS1-FLAG
IP: WFS1-FLAG
IB: FLAG-FLII
IP: FLAG-FLII
IB: myc-CD2AP
IP: myc-CD2AP
IB: myc-PKD2
IP: myc-PKD2
IB: FLAG-CAMK2D
IP: FLAG-CAMK2D
p-Akt(S473)
pan-Akt
E
IB: myc-INTS3
IP: myc-INTS3
IB: myc-CABLES1
IP: myc-CABLES1
IB: myc-PERK
IP: myc-PERK
IB: FLAG-HSPA8
IP: FLAG-HSPA8
IB: FLAG-BCL10
IP: FLAG-BCL10
IB: FLAG-PKD1
IP: FLAG-PKD1
IB: FLAG-CALPAIN1
IP: FLAG-CALPAIN1
IB: HA-ATRX
IP: HA-ATRX
F
YAP1 wt
YAP1 S109A
MK 2206
IB: FLAG-YAP1
IP: FLAG-YAP1
INTS3 wt
INTS3 S1034A
HSPA8 wt
HSPA8 S285A
IB: GFP-HSPA8
IP: GFP-HSPA8
ATRX wt
ATRX S785A
BCL10 wt
BCL10 T52A
G
IB: FLAG-HSPA8
IP: anti-RxRxxS*/T*
FLAG-HSPA8
IB: FLAG-Bcl10
FLAG-Bcl10
IB: FLAG-PKD1
FLAG-PKD1
pLenti-GFP
EMSY wt
EMSY S209A
IB: FLAG-EMSY
IP: FLAG-EMSY

Figure S1 (related to fig 1): The phosphoproteomes of Akt1, Akt2, Akt3 and Akt1/2/3-expressing cells.

(A) Schematic representation of the protocol we used to generate mouse lung fibroblast lines expressing different Akt isoforms. These cells exhibit significant biological differences (Ezell et al., 2012; Iliopoulos et al., 2009; Polytarchou et al., 2011) despite the fact that the three Akt isoforms have similar domain composition and very high sequence homology and structural similarity (Huang et al., 2003; Kumar and Madison, 2005; Scheid and Woodgett, 2001; Wu et al., 2010; Yang et al., 2002).

(B) Distribution of the robust z scores of all phosphorylation events in Akt1, Akt2, Akt3 and Akt1/2/3 cells. Combined data from three separate experiments.

(C) Validation of novel Akt targets. (Left panels) Lung fibroblasts expressing Akt1, Akt2 or Akt3 were treated with Akt inhibitors MK2206 or AZD5363. Cell lysates from inhibitor or DMSO-treated cells, harvested after 30 minutes of treatment, were used for immunoprecipitation with HGK or PRAS40 antibodies. The immunoprecipitates were probed with the Akt phosphosubstrate antibody, or with the HGK or PRAS40 antibodies as indicated. (Right panels) Western blots of cell lysates from the same cells were probed with phospho-DNAJC2, phospho-PRAS40, DNAJC2 and PRAS40 antibodies, as indicated.

(D-E) HEK293 cells were transfected with the indicated epitope-tagged constructs, and the transfected cells were treated with the Akt inhibitors MK2206 or AZD5363. Using anti-epitope tag antibodies, the proteins expressed from these constructs were immunoprecipitated and the immunoprecipitates were probed with the Akt phosphosubstrate antibody, or with an antibody that detects the protein independent of its phosphorylation status (loading control) as indicated. To monitor the inhibition of Akt, western blots of cell lysates were probed with phosho-Akt (S473) and pan-Akt antibodies (D) or with phospho-PRAS40 (T246) and total-PRAS40 antibodies (positive control) as indicated (E).

(F) HEK293 cells were transfected with the indicated epitope-tagged constructs (wild type or phosphorylation site mutants). The proteins expressed from these constructs, were immunoprecipitated and the immunoprecipitates were probed with the Akt phosphosubstrate antibody, or with an antibody that detects the protein independent of its phosphorylation status, as in D.

(G) Akt1, Akt2, or Akt3-expressing lung fibroblasts, were transduced with the indicated constructs. As in D and E, the proteins expressed from these constructs were immunoprecipitated and the immunoprecipitates were probed with the indicated antibodies.

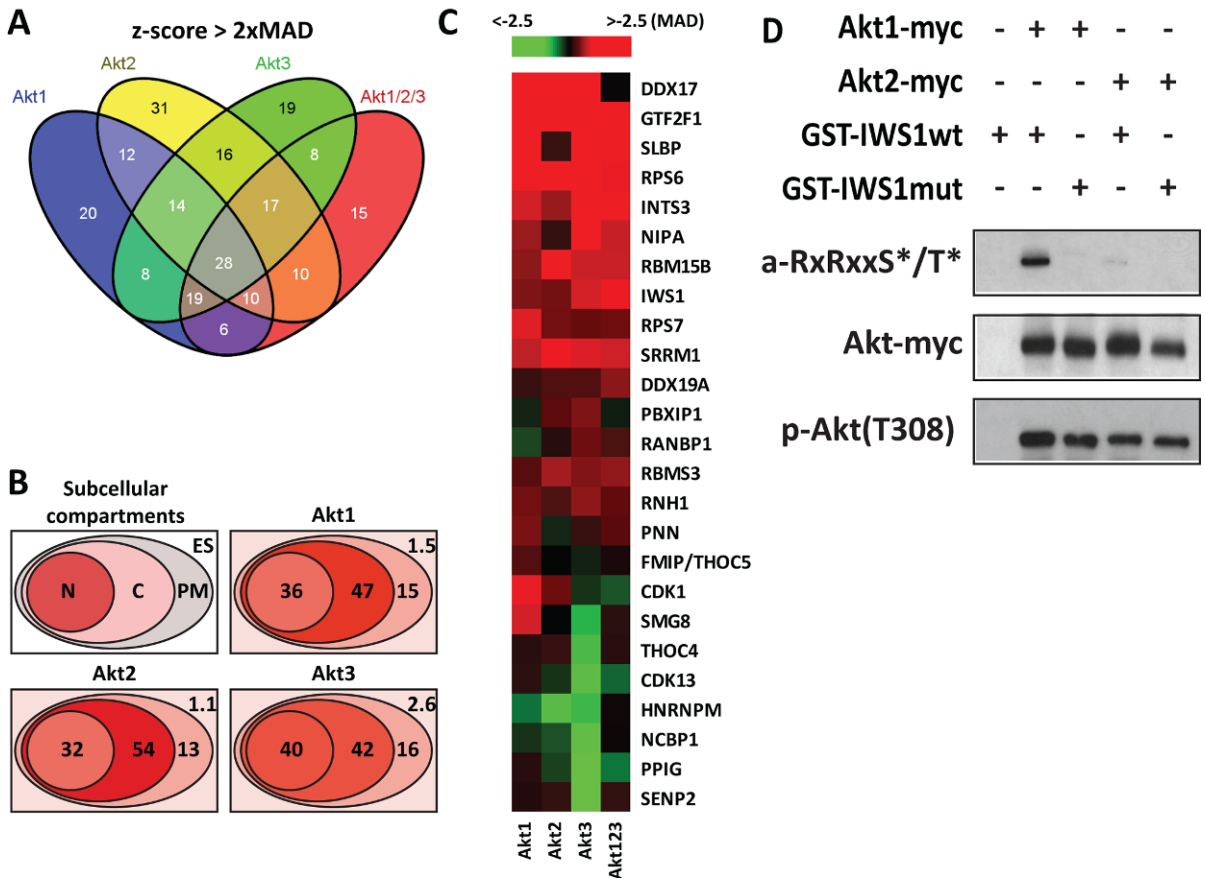

Figure S2 (related to fig 2): Akt1, Akt2 and Akt3 phosphorylation targets and their subcellular distribution. Phosphorylation of proteins involved in RNA metabolism and differential phosphorylation of IWS1 by Akt1 and Akt2.

(A) Venn diagram showing the Akt isoforms responsible for all the phosphorylation events with robust z-score 2 MAD values or more above the median.

(B) Subcellular localization of the proteins phosphorylated by Akt1, Akt2, or Akt3. The numbers indicate the percentage of Akt1, Akt2 or Akt3 phosphorylation targets that are localized in the plasma membrane (PM), the cytoplasm (C), the nucleus (N), or the extracellular space (ES). The phosphorylation targets of each Akt isoform were identified based on phosphorylation events with a robust z score, 2 MAD values or more above the median.

(C) Heat map of the abundance of phosphorylation of the Akt-mediated phosphorylation events of proteins involved in RNA processing. For some proteins, the abundance of phosphorylation is high

in cells expressing a single Akt isoform, but low in Akt1/2/3 cells (see also Fig 1C). This phenomenon may be due to the functional inhibition of one Akt isoform by another, which had been suggested by earlier studies (Iliopoulos et al., 2009; Irie et al., 2005). Alternatively, Akt isoforms may differentially regulate feedback loops that control the phosphorylation of specific Akt targets.

(D) In vitro kinase assay of myc-tagged Akt1 and Akt2, using GST-IWS1wt and GST-IWS1 S720A/T721A recombinant proteins as substrates. Myc-Akt1 and myc-Akt2 were immunoprecipitated with the anti-myc antibody. Phosphorylation was detected with the Akt phosphosubstrate antibody (a-RxRxxS*/T*). Western blots of the same lysates were probed with the anti-myc antibody (Akt-myc) (loading control), and the anti-phosphoThr308-Akt antibody, as indicated. These results compliment the data in figure 2H which, in addition to the phosphorylation of the wild type IWS1 and IWS1-S720A/T721A substrates, also addressed the phosphorylation of the IWS1-S720A and IWS1-T721A substrates by Akt1. The mutation of either of these sites abrogated the phosphorylation of IWS1 by Akt in vitro. This finding is in agreement with the observation that both Ser720 and Thr721 undergo phosphorylation in the Akt -expressing cells. However, the Akt phosphosubstrate antibody, which recognizes the phosphorylated RXRXXS motif, should detect only the phosphorylated Ser residue. Therefore, the lack of detection of the IWS1-S720A mutant substrate in the in vitro kinase assay shows that Akt indeed phosphorylates this site. The lack of detection of the IWS1-T721A mutant on the other hand, suggests that the mutation of the Thr residue interferes with the phosphorylation of the Ser residue, perhaps because the Ser and Thr phosphorylations are functionally linked.

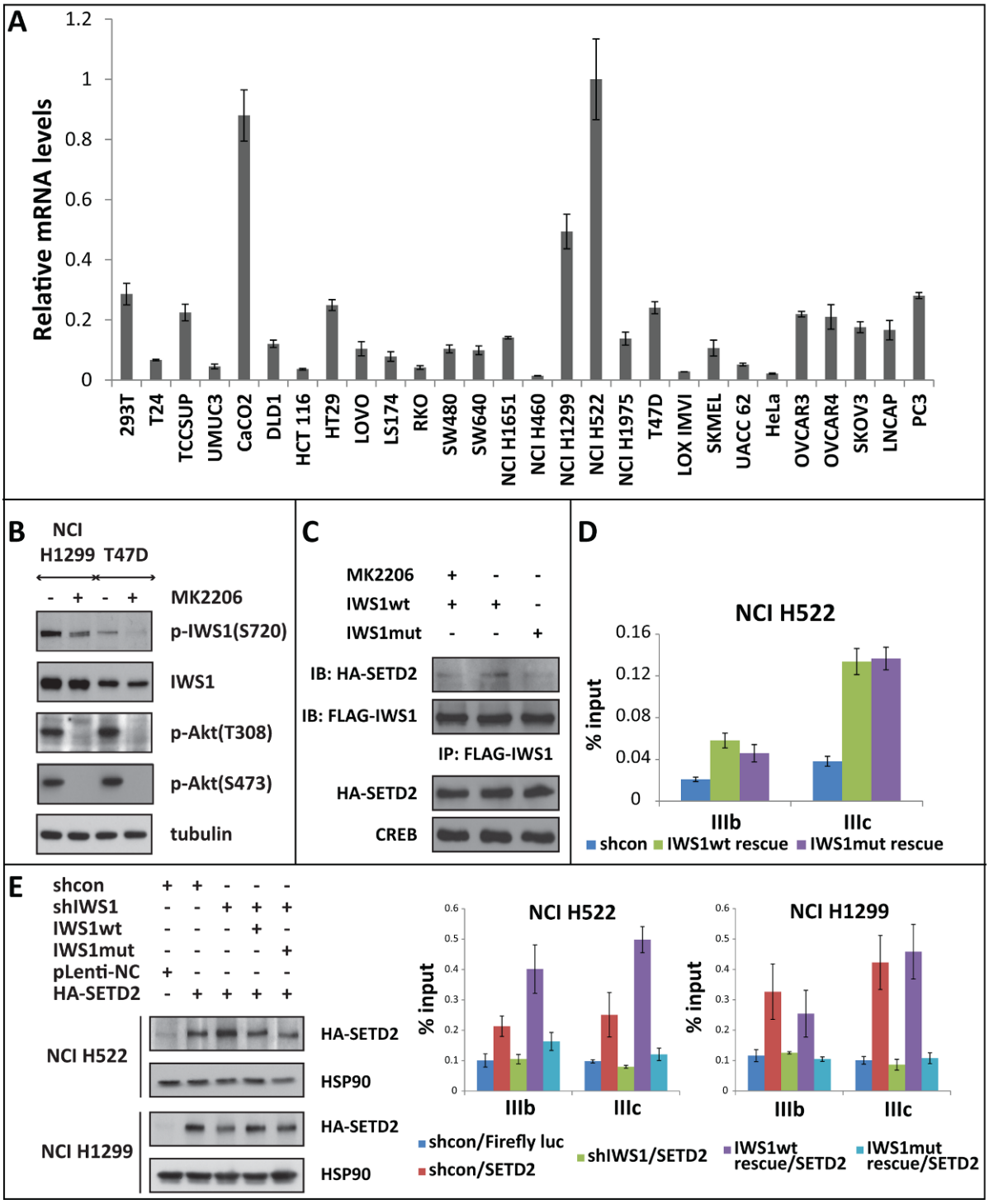

Figure S3 (related to fig 3): IWS1 is expressed and phosphorylated in cancer cell lines and co-immunoprecipitates with SetD2. Flag-IWS1 and HA-SetD2 binding to the FGFR-2 gene.

(A) Relative IWS1 mRNA levels in the indicated tumor cell lines were measured with real time RT-PCR. *GAPDH* was used as the control. The expression of IWS1 in NCI H522, NCI H1299 and T47D cells was also measured by western blotting (see figure 3A).

(B) The Akt inhibitor MK2206 inhibits the phosphorylation of IWS1 at Ser720/Thr721 as determined by western blotting with a non-commercially available antibody from Cell Signaling. Western blots of cell lysates of NCI H1299 and T47D cells, harvested after (2 hours) treatment with MK2206 or DMSO, were probed with the indicated antibodies. The incomplete inhibition of IWS1 phosphorylation in NCI H1299 cells may be caused by the slow IWS1 dephosphorylation kinetics in this cell line. Alternatively, it may be due to phosphorylation by another kinase that targets the Akt phosphorylation consensus and is active in these cells. However, this seems unlikely because the knockdown of Akt isoforms or inhibition with Akt specific inhibitors in these cells have profound effects on the biology elicited by IWS1 phosphorylation.

(C) Upper panels: shIWS1/wt rescue and shIWS1/mutant rescue NCI H1299 cells were transduced with an HA-SETD2 construct and they were treated with MK2206 or DMSO, as indicated. FLAG-IWS1 was immunoprecipitated from cell lysates harvested at 2 hours after the treatment, and the immunoprecipitates were probed with the HA-tag or FLAG-tag (control) antibodies. Lower panels: Cell lysates were probed with HA-tag and CREB antibodies (Input).

(D) Both the wild type IWS1 and its phosphorylation site mutant bind exons IIIb and IIIc of the FGFR-2 gene. Data in the ChIP experiment in figure 3G were recalculated and presented as percentage of the input.

(E) HA-SetD2 binds the IIIb and IIIc exons of FGFR-2 in shIWS1/wt rescue but not in shIWS1/mutant rescue NCI H522 and NCI H1299 cells. Left panel: Western blots of cell lysates derived from shControl, shIWS1, shIWS1/wt rescue and shIWS1/mutant rescue NCI H522 and NCI H1299 cells, transduced with lentiviral constructs of SetD2 or firefly luciferase (negative control), were probed with anti-HA and anti-HSP90 (loading control) antibodies, as

indicated. The lysates were derived from the cells in the experiments in figures 3H and 3I. (Middle and Right panels) Data in the ChIP experiment in figures 3H and 3I were recalculated and presented as percentage of the input.

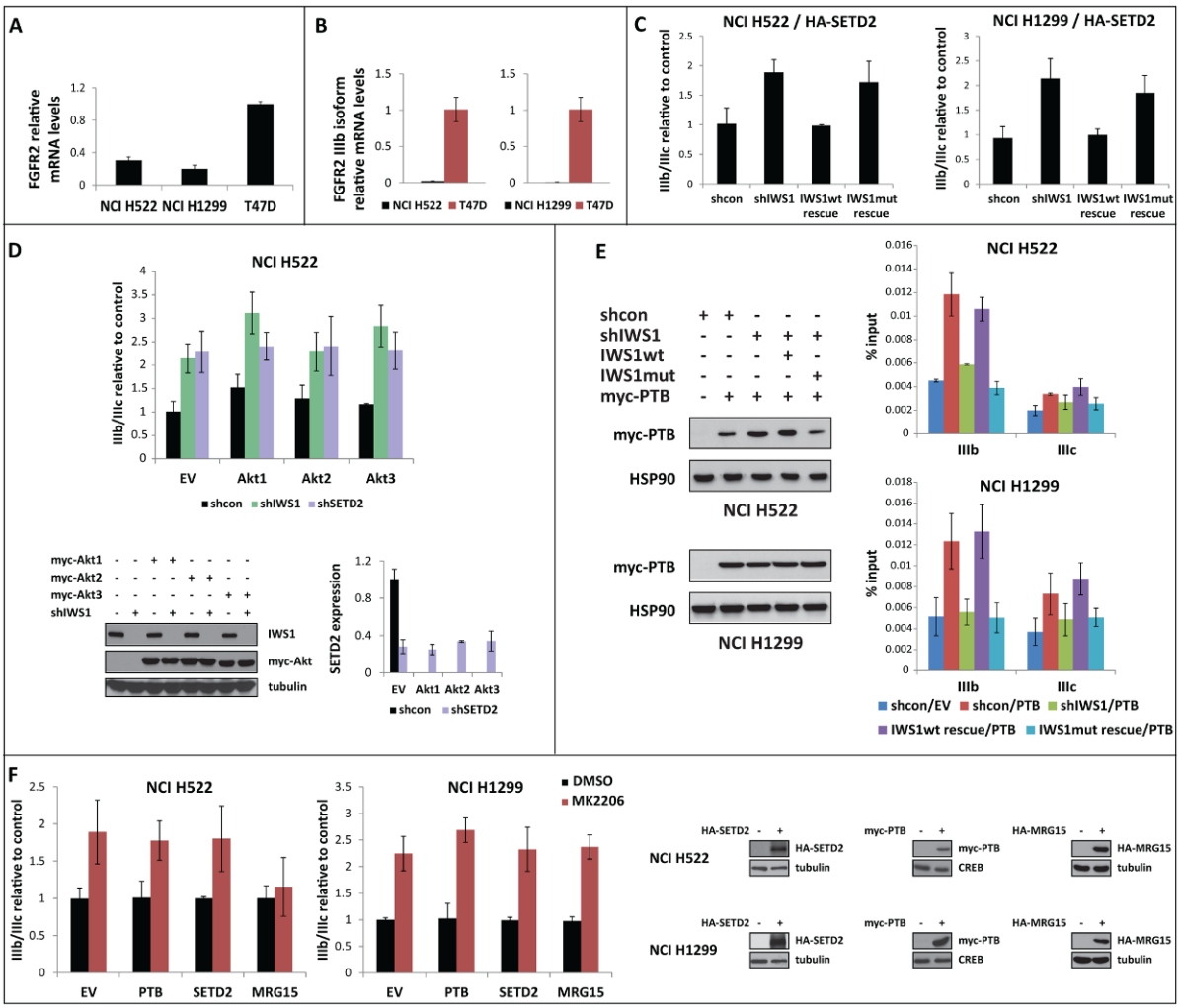

Figure S4 (related to fig 4): IWS1 phosphorylation at Ser720/Thr721 by Akt3 and Akt1 regulates the alternative splicing of the *FGFR-2* gene. Exogenous PTB expression in myc-PTB transduced cells.

(A and B) Expression of total *FGFR-2* and *FGFR-2* IIIb in NCI H522, NCI H1299 and T47D cells. (A) Relative mRNA levels of *FGFR-2* in NCI H522, NCI H1299 and T47D cells were measured by real time RT PCR. *GAPDH* was used as the control. (B) Relative mRNA levels of the *FGFR-2* IIIb transcript in NCI H522, NCI H1299 and T47D cells were measured by real time RT PCR. *GAPDH* was used as the control.

(C) Overexpression of SetD2 failed to rescue the shIWS1 and shIWS1/mutant rescue *FGFR-2* alternative splicing phenotype. Real time RT-PCR showing the ratio of the IIIb/IIIc isoforms in

the cells used for the experiments in figures 3H, 3I and S3C (shControl, shIWS1, shIWS1/wt rescue and shIWS1/mutant rescue NCI H522 and NCI H1299 cells transduced with an HA-SETD2 construct). Bars show the mean IIIb/IIIc ratio in shIWS1, shIWS1/wt rescue and shIWS1/mutant rescue cells, relative to shControl cells ± SD.

(D) Overexpression of Akt1, Akt2 or Akt3 failed to rescue the shIWS1-induced *FGFR-2* alternative splicing phenotype. NCI H522 cells were transduced with retroviral constructs expressing myc-Akt1, myc-Akt2, myc-Akt3, or with the empty vector (EV). Following this, the cells were transduced with shcon, shIWS1 or shSETD2 constructs and they were analyzed by real time RT-PCR for the ratio of the *FGFR-2* IIIb/IIIc isoforms. (Upper panel): Bars show the mean IIIb/IIIc ratio relative to EV/shControl cells ± SD; (Left, lower panel) Cell lysates from the same cells were probed with the indicated antibodies. (Right, lower panel) SETD2 expression levels were measured by real time RT-PCR relative to EV/shControl cells ± SD.

(E) Myc-PTB binds the IIIb and IIIc exons of *FGFR-2* in shIWS1/wt rescue but not in shIWS1/mutant rescue NCI H522 and NCI H1299 cells. (Left panel) PTB expression in myc-PTB transduced cells. Cell lysates were derived from shControl, shIWS1, shIWS1/wt rescue and shIWS1/mutant rescue NCI H522 and NCI H1299 cells transfected with a construct of myc-PTB. Western blots of these lysates were probed with anti-myc and anti-HSP90 (loading control) antibodies, as indicated. (Right panel): The cells in the left panel were used for the experiment in figures 4G and 4H. Data in the ChIP experiment in these figures were recalculated and presented as percentage of the input.

(F) SetD2, PTB and MRG15 failed to rescue the *FGFR-2* alternative splicing phenotype in NCI H522 and NCI H1299 cells treated with MK2206. NCI H522 and NCI H1299 cells were transfected with HA-SETD2, myc-PTB, or HA-MRG15 expression constructs or with the empty vector (EV). The transfected cells were treated with the Akt inhibitor MK2206, or with DMSO. (Left panel) The *FGFR-2* IIIb/IIIc ratio in cells transfectd with each of the constructs and treated either with MK2206 or DMSO was measured by real time RT-PCR. Bars show the mean IIIb/IIIc

ratio relative to untreated (DMSO-treated) cells ± SD. (Right panel): Cell lysates derived from the cells in the left panel were probed with the indicated antibodies.

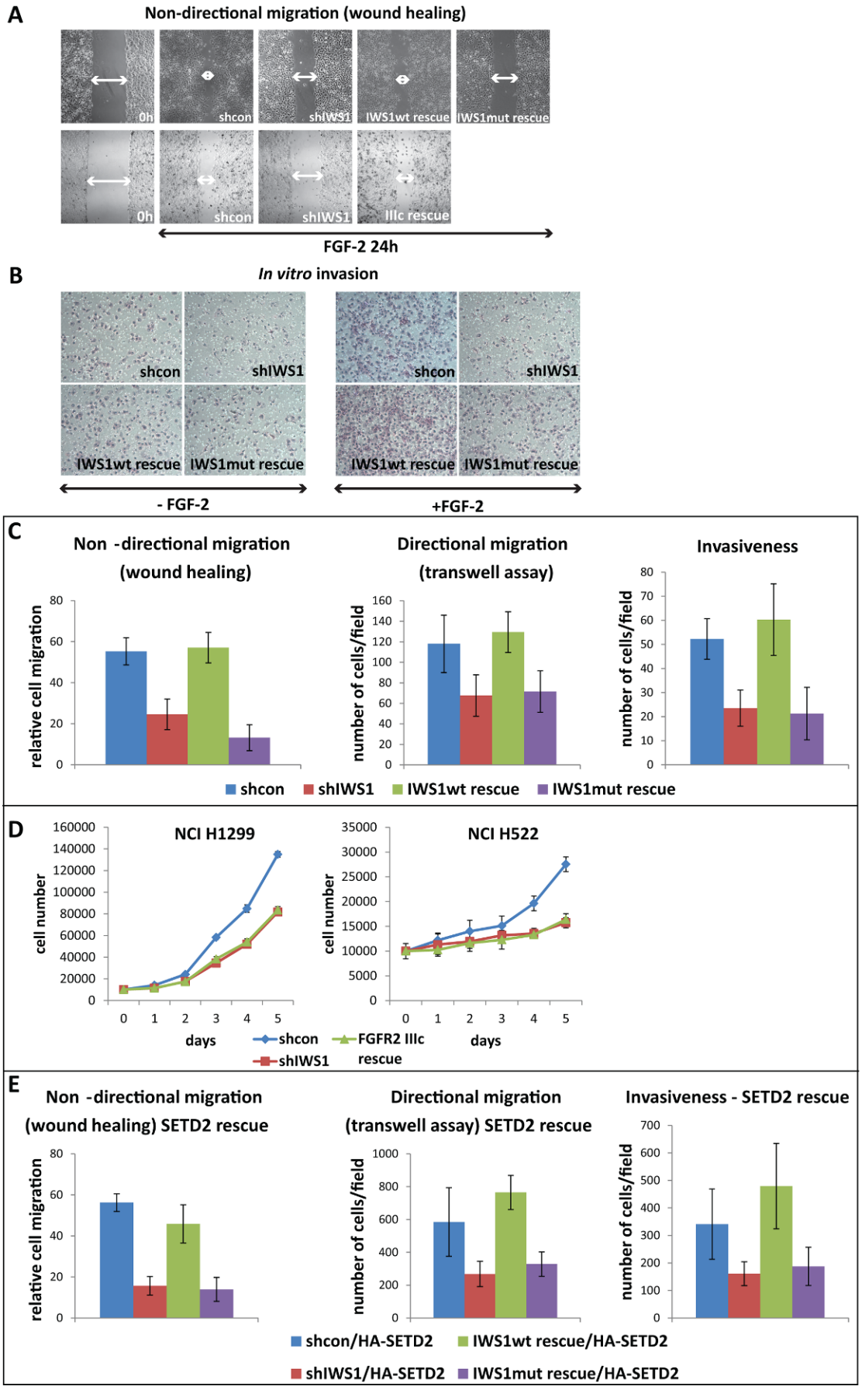
A
Non-directional migration (wound healing)
0h
shcon
shIWS1
IWS1wt rescue
IWS1mut rescue
0h
shcon
shIWS1
IIIc rescue
FGF-2 24h
B
In vitro invasion
shcon
shIWS1
IWS1wt rescue
IWS1mut rescue
shcon
shIWS1
IWS1wt rescue
IWS1mut rescue
- FGF-2
+FGF-2
C
Non -directional migration (wound healing)
relative cell migration
Directional migration (transwell assay)
number of cells/field
Invasiveness
number of cells/field
shcon
shIWS1
IWS1wt rescue
IWS1mut rescue
D
NCI H1299
cell number
days
NCI H522
cell number
days
shcon
shIWS1
FGFR2 IIIc rescue
E
Non -directional migration (wound healing) SETD2 rescue
relative cell migration
Directional migration (transwell assay) SETD2 rescue
number of cells/field
Invasiveness - SETD2 rescue
number of cells/field
shcon/HA-SETD2
IWS1wt rescue/HA-SETD2
shIWS1/HA-SETD2
IWS1mut rescue/HA-SETD2

Figure S5 (related to fig 6): IWS1 phosphorylation at Ser720/Thr721 in lung carcinoma cell lines promotes cell migration, invasiveness and proliferation.

(A) Expression of the IIIc isoform of *FGFR-2* is sufficient to rescue cell migration of shIWS1 NCI H1299 cells. (Upper panels) Wound healing assays were carried out on monolayers of confluent cultures of shControl, shIWS1, shIWS1/wt rescue and shIWS1/mutant rescue NCI H1299 cells. (Lower panels) Wound healing assay of shControl and shIWS1 NCI H1299 cells. The latter cells were either rescued with a lentiviral contruct of the IIIc isoform of *FGFR-2*, or they were not rescued, as indicated.

(B) Invasion of NCI H1299 cells into FGF-2-supplemented matrigel depends on the phosphorylation of IWS1. shControl, shIWS1, shIWS1/wt rescue and shIWS1/mutant rescue NCI H1299 cells were plated in FGF-2-deficient matrigel (Left panels), or supplemented with FGF-2-supplemented matrigel (Right panels). Cell invasion of the matrigel was monitored by light microscopy.

(C) IWS1 phosphorylation is required for cell migration and invasiveness, not only in NCI H1299 cells (fig 6A, 6B, 6C, S5A and S5B), but also in NCI H522 cells. Wound healing, directional migration and cell invasiveness assays were carried out in shControl, shIWS1, shIWS1/wt rescue and shIWS1/mutant rescue NCI H522 cells, growing in serum-free media supplemented with FGF-2. Results are presented as in figures 6A, 6B and 6C.

(D) Growth curves of shControl and shIWS1 NCI H1299 cells (left panel) or NCI H522 cells (right panel) growing in media supplemented with 10% FBS. The impaired proliferation in shIWS1 cells was not-rescued by *FGFR-2* IIIc isoform.

(E) Overexpression of SetD2 failed to rescue the cell migration and invasion defects in shIWS1 and shIWS1/mutant rescue cells. Non-directional migration, directional migration and cell invasiveness assays were carried out in shControl, shIWS, shIWS1/wt rescue and shIWS1/mutant rescue NCI H1299 cells transduced with an HA-SETD2 construct and growing

in serum-free media supplemented with FGF-2. Results are presented as in figures 6A, 6B and 6C. Therefore, the regulation of cell migration and invasion by SetD2 depends on the phosphorylation of IWS1.

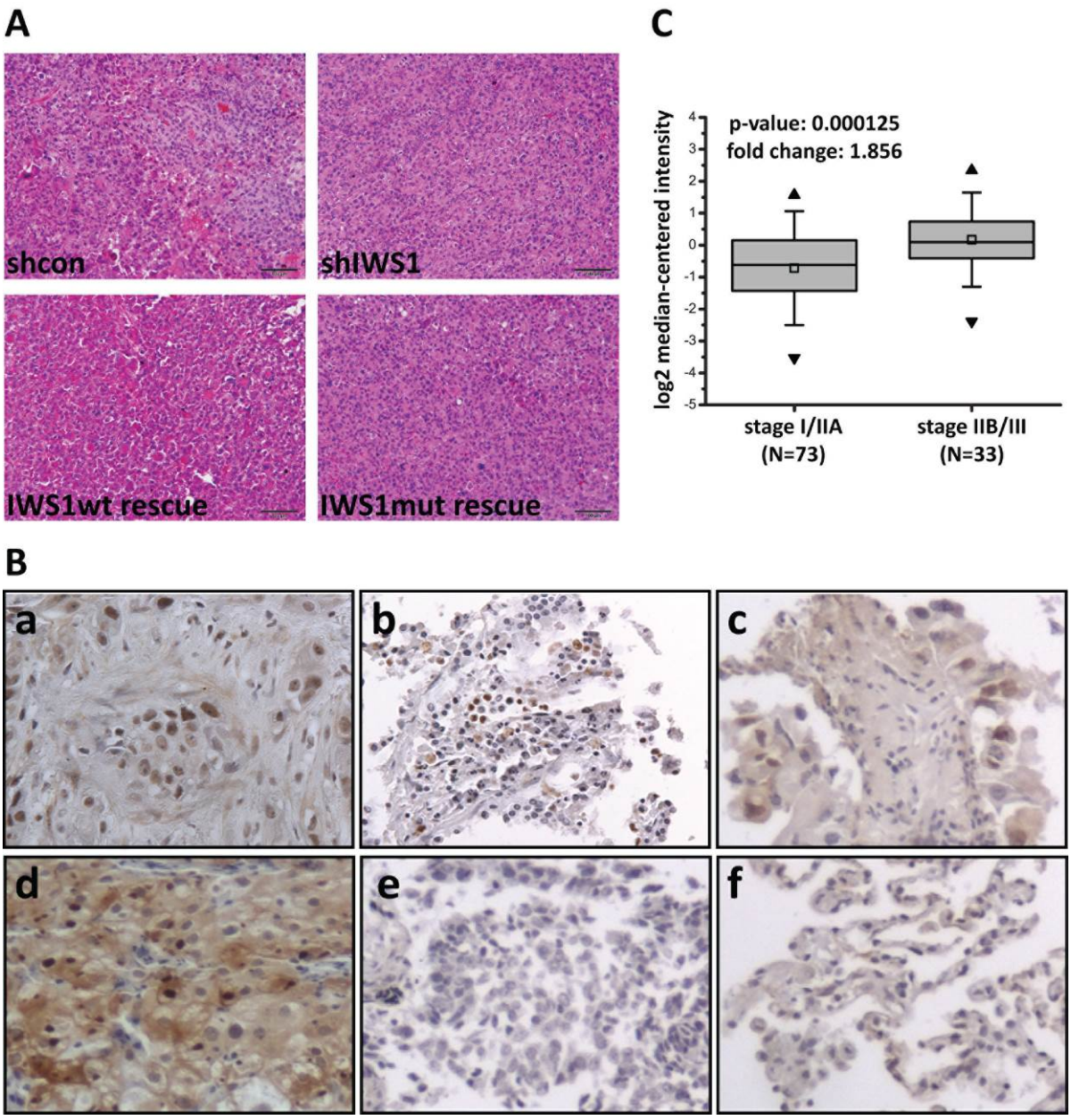

Figure S6 (related to fig 7): IWS1 phosphorylation at Ser720/Thr721 in NSCLC.

(A) Histology of the tumors arising in nude mice injected subcutaneously with shControl, shIWS1, shIWS1/wt rescue or shIWS1/mutant rescue NCI H1299 cells. Sections were stained with Hematoxylin and Eosin.

(B) Immunohistochemical staining of normal human lung and lung cancer specimens with the anti-phospho-IWS1 (Ser720) antibody. Representative pictures of positively staining squamous

cell carcinomas (a and b) and adenocarcinomas (c and d). (v) Negatively staining adenocarcinoma and (e) normal lung tissue (f).

(C) Data from the Oncomine database suggest that the expression of IWS1 correlates with the tumor stage in lung cancer, with tumors at a more advanced stage expressing higher IWS1 levels.

SUPPLEMENTARY TABLES

	Phosphorylation site (human)	References
ACLY	S455	(Berwick et al., 2002)
B-RAF	S429	(Guan et al., 2000)
BRCA1	S694	(Nelson et al., 2010)
CaRHSP1	S52	(Auld et al., 2005)
CCT2	S260	(Abe et al., 2009)
EDC3	S161	(Larance et al., 2010)
eIF4B	S422	(van Gorp et al., 2009)
EMSY	S209	(Ezell et al., 2012)
FLNC	S2233	(Murray et al., 2004)
FoxO1a	S256	(Biggs et al., 1999; Rena et al., 1999)
FoxO3a	S253	(Brunet et al., 1999; Brunet et al., 2001)
GOLGA3	S389	(Ran et al., 2007)
GSK-3a	S21	(Cross et al., 1995; Somervaille et al., 2001)
H2B	S37	(Alessi et al., 1996)
HMOX1	S188	(Salinas et al., 2004)
HtrA2	S212	(Yang et al., 2007)
Lamin A/C	S301, S404	(Cenni et al., 2008)
MAPKAP1	T86	(Humphrey et al., 2013)
MDM2	S186	(Mayo and Donner, 2001)
mTOR	S2448	(Nave et al., 1999)
MYO5A	S1652	(Yoshizaki et al., 2007)
NEDD4L	S342, S448	(Lee et al., 2007)
NDRG2	T348	(Burchfield et al., 2004)
PDCD4	S67	(Palamarchuk et al., 2005)
PEA15	S116	(Trencia et al., 2003)
PFKFB2	S483	(Bertrand et al., 1999; Deprez et al., 1997; Mouton et al., 2007)
PRAS40	T246	(Kovacina et al., 2003)
RANBP3	S126	(Yoon et al., 2008)
S6	S235, S236	(Chiu et al., 2005; Zhang et al., 2002)
SEK1	S80	(Park et al., 2002; Song and Lee, 2005)
Tsc2	S981	(Cai et al., 2006; Inoki et al., 2002; Manning et al., 2002; Roux et al., 2004)
TBC1D1	T596	(Chen et al., 2008)
WNK1	T60	(Vitari et al., 2004; Xu et al., 2005)

Table S1: Akt substrates that had been identified previously and were confirmed by this screen.

Cell type	Growth medium
HEK293T	DMEM high glucose, 10% FBS, P/S, non-essential amino acids, L-glutamine
T24	McCoy's 5a Medium modified, 10% FBS, P/S, non-essential amino acids, L-glutamine
TCCSUP	RPMI 1640, 10% FBS, P/S, non-essential amino acids, L-glutamine
UMUC3	RPMI 1640, 10% FBS, P/S, non-essential amino acids, L-glutamine
CACO2	MEM, 10% FBS, P/S, non-essential amino acids, L-glutamine
DLD1	RPMI 1640, 10% FBS, P/S, non-essential amino acids, L-glutamine
HCT116	DMEM high glucose, 10% FBS, P/S, non-essential amino acids, L-glutamine
HT29	DMEM high glucose, 10% FBS, P/S, non-essential amino acids, L-glutamine
LOVO	DMEM high glucose, 10% FBS, P/S, non-essential amino acids, L-glutamine
LS174	MEM, 10% FBS, P/S, non-essential amino acids, L-glutamine
RKO	MEM, 10% FBS, P/S, non-essential amino acids, L-glutamine
SW480	DMEM high glucose, 10% FBS, P/S, non-essential amino acids, L-glutamine
SW640	DMEM high glucose, 10% FBS, P/S, non-essential amino acids, L-glutamine
NCI H1651	RPMI 1640, 10% FBS, P/S, non-essential amino acids, L-glutamine
NCI H460	RPMI 1640, 10% FBS, P/S, non-essential amino acids, L-glutamine
NCI H1299	RPMI 1640, 10% FBS, P/S, non-essential amino acids, L-glutamine
NCI H522	RPMI 1640, 10% FBS, P/S, non-essential amino acids, L-glutamine
NCI1975	RPMI 1640, 10% FBS, P/S, non-essential amino acids, L-glutamine
T47D	RPMI 1640, 10% FBS, P/S, non-essential amino acids, L-glutamine
LOXMVII	RPMI 1640, 10% FBS, P/S, non-essential amino acids, L-glutamine
SKMEL	RPMI 1640, 10% FBS, P/S, non-essential amino acids, L-glutamine
UACC62	RPMI 1640, 10% FBS, P/S, non-essential amino acids, L-glutamine
HeLa	DMEM high glucose, 10% FBS, P/S, non-essential amino acids, L-glutamine
OVCAR3	RPMI 1640, 10% FBS, P/S, non-essential amino acids, L-glutamine
OVCAR4	RPMI 1640, 10% FBS, P/S, non-essential amino acids, L-glutamine
SKOV3	RPMI 1640, 10% FBS, P/S, non-essential amino acids, L-glutamine
LNCAP	RPMI 1640, 10% FBS, P/S, non-essential amino acids, L-glutamine
PC3	RPMI 1640, 10% FBS, P/S, non-essential amino acids, L-glutamine

Table S2: Growth media for human cancer cell lines.

constructs	
pCMV-myc-PTB1	Addgene plasmid 23024 (Xie et al., 2003)
pMSCV-FlagBcl10	Addgene plasmid 18718 (Wu and Ashwell, 2008)
pBABE YAP1	Addgene plasmid 15682 (Overholtzer et al., 2006)
pWZL Neo Myr Flag CAMK2D	Addgene plasmid 20440 (Boehm et al., 2007)
WFS1-Flag-pcDNA3	Addgene plasmid 13011 (Fonseca et al., 2005)
pWZL Neo Myr Flag UCK2	Addgene plasmid 20661 (Boehm et al., 2007)
M-PKD2 (OF2-3)	Addgene plasmid 21370 (Hanaoka et al., 2000)
pCI-PKD1-Flag	Addgene plasmid 21369 (Hanaoka et al., 2000)
CMV-GFP-NMHC II-A	Addgene plasmid 11347 (Wei and Adelstein, 2000)
pcDNA5/FRT/TO GFP HSPA8	Addgene plasmid 19487 (Hageman and Kampinga, 2009)
pBabe-puro-PERK-myc	Kind offer from Dr. David Ron (Addgene plasmid 21819)
pCDNA 3.1 myc-CD2AP	Kind offer from Dr. Andrey Shaw (Department of Pathology & Immunology, School of Medicine, Washington University in St. Louis) (Dustin et al., 1998)
pCDNA 3 FLAG-FLIl	Kind offer from Dr. Michael R. Stallcup (Biochemistry and Molecular Biology, Keck School of Medicine, University of Southern California) (Lee et al., 2004)
pDEST-myc-INTS3	Kind offer from Dr. Junjie Chen (The University of Texas MD Anderson Cancer Center) (Huang et al., 2009)
pEGFP-HA-ATRX	Kind offer from Dr. David Picketts (Ottawa Hospital Research Institute) (Tang et al., 2004)
pGEX-IWS1	Kind offer from Dr. Jones KA lab (The Salk Institute for Biological Studies, La Jolla, California, USA) (Yoh et al., 2007)
pcDNA3.1-MRG15-HA	Kind offer from Dr. Kaoru Tominaga (Jichi Medical University, 3311-1 Yakushiji, Shimotsuke, Tochigi, Japan) (Tominaga et al., 2003)
pCR-XL-TOPO-SETD2	Open Biosystems (cat. no. MHS4426-99240353, clone ID 40125713)
pBabe-puro-FGFR2 IIIb isoform	Addgene plasmid 45698 (Liao et al., 2013)
pDONR-FGFR2 transcript variant 1 (IIIc)	GeneCopoeia (cat. no. GC-A0979)

pOTB7-CAPN1	3629894 (ATCC® 10658559™)
pCMV-SPORT6-CABLES1	5196987 (ATCC® MGC-35496™)
pENTR/D-TOPO cloning vector	Invitrogen, cat. no. 45-0218
pLenti CMV Puro DEST	Addgene, cat. no. 17452 (Campeau et al., 2009)
pLenti CMV Neo DEST	Addgene, cat. no. 17392 (Campeau et al., 2009)

siRNAs	
siRNA negative control	Ambion, cat. no. AM4611
siRNA against AKT1	Ambion, cat. no. s659
siRNA against AKT2	Ambion, cat. no. s1217
siRNA against AKT3	Ambion, cat. no. s19428

shRNAs	
Non-silencing-GIPZ lentiviral shRNAmir control	Open Biosystems, cat. no. RHS4346
shRNA against human IWS1	Open Biosystems, cat. no. RSH4430-101101545, clone ID V3LHS_389019
pLKO.1 empty vector control	Open Biosystems, cat. no. RSH4080
shRNAs against human SETD2	Open Biosystems, cat. no. RSH3979-9571647, clone ID TRCN0000003029 and Open Biosystems, cat. no. RSH3979-9571650, clone ID TRCN0000003032

Table S3: Constructs, siRNAs and shRNAs

Primers for IWS1, SETD2, CALPAIN1 and CABLES1 constructs		
	Forward	**Reverse**
IWS1 with FLAG-tag	CACCATGGATTATAAAGATGATGATGATAAAGACTCGGAATATTACAGCGGCGAC	TCACAATGGCATTTTGTTGCCC
SETD2 with HA-tag	CACCATGTATCCTTACGACGTGCCCGATTATGCCGAAAGAAGAGGCAAGTATTCTTCAAA	TCACTCTAATTCAGTGTCCTCTTTTGG
CALPAIN1 with FLAG-tag	CACCATGGATTATAAAGATGATGATGATAAATCGGAGGAGATCATCACGC	TCATGCAAACATGGTCAGCTG
CABLES1 with myc-tag	CACCATGGAGCAGAAGCTGATCAGCGAGGAGGACCTGCTTTCTAAGAGGGGCTGCCAT	CTAGGAACTCTGGACCAGCCG

Mutagenesis Primers		
	Forward	**Reverse**
IWS1 (S720A)	CAACGACGAAGAATGAACGCCACTGGTGGTCAGACACC	GGTGTCTGACCACCAGTGGCGTTCATTCTTCGTCGTTG
IWS1 (T721A)	ACGAAGAATGAACAGCGCTGGTGGTCAGACACC	GGTGTCTGACCACCAGCGCTGTTCATTCTTCGT
IWS1 (S720A,T721A)	CAACGACGAAGAATGAACGCCGCTGGTGGTCAGACACCCA	TGGGTGTCTGACCACCAGCGGCGTTCATTCTTCGTCGTTG
IWS1 (S720D, T721E)	GCCTCAACGACGAAGAATGAACGACGAGGGTGGTCAGACACCCAGAAGAG	CTCTTCTGGGTGTCTGACCACCCTCGTCGTTCATTCTTCGTCGTTGAGGC
IWS1-shRNA resistant mutant	AGCATAGTGGGATTGGACGCGCGGTCATGTACCTCTATAAACACCCCAAGG	CCTTGGGGTGTTTATAGAGGTACATGACCGCGCGTCCAATCCCACTATGCT
HSPA8 (T265A)	GTAAGACGCCTCCGTGCTGCTTGTGAACGTG	CACGTTCACAAGCAGCACGGAGGCGTCTTAC
ATRX (S785A)	AAAAGGAAACGAAAAAGTTCTGCATCTGGCTCAGATTTTGATA	TATCAAAATCTGAGCCAGATGCAGAACTTTTTCGTTTCCTTTT
BCL10 (T52A)	AAAAATACTCAGTAGAGAAGACGCTGAAGAAATTTCTTGTCGAAC	GTTCGACAAGAAATTTCTTCAGCGTCTTCTCTACTGAGTATTTTT
INTS3 (S1034A)	GGAAACGAAAAGGGGCCTCTGCA	GCCCACTGCAGAGGCCCCTTTT

	GTGGGC	CGTTTCC
YAP1 (S109A)	CACTCCCGACAGGCCGCTACTGATGCAGGCAC	GTGCCTGCATCAGTAGCGGCCTGTCGGGAGTG

Real Time PCR primers			
	Forward	**Reverse**	**Product size (bp)**
h*GADPH*	TTCGACAGTCAGCCGCATCTTCTT	CAGGCGCCCAATACGACCAAATC	110
h*IWS1*	GAACAGCACTGGTGGTCAGACACC	AGGCATTGGGACCCTTGCACG	118
h*SETD2*	AGCTCCCTCTCACCACCCTCTT	CAACTTCCGGCGTTCCTCTGT	138
h*FGFR-2* (e6)	TCCATCAATCACACGTACCACCTG	ACTCTACGTCTCCTCCGACCACTG	112
h*FGFR-2* (IIIb)	AAGTGCTGGCTCTGTTCAATGT	GTAGTCTGGGGAAGCTGTAATCTC	161
h*FGFR-2* (IIIc)	TGAGGACGCTGGGGAATATACG	TAGTCTGGGGAAGCTGTAATCTCCT	123

ChIP primers			
	Forward	**Reverse**	**Product size (bp)**
***FGFR-2* (TSS)**	GGCAACCCTCCCCGCAGTATCAAG	GCTGGCCAACGGCTCGCTGAG	139
***FGFR-2* (IIIb)**	AGCCCTTTAATGCCGCTGTTTAGA	TAACGGCCAACCAGGAAGGTCTTAG	102
***FGFR-2* (IIIc)**	GAATATACGTGCTTGGCGGGTAAT	TAAAAGGGGCCATTTCTGATAACA	166
***GAPDH* (e3)**	AGGTGGCCTAGGGCTGCTCACATA	GGCGCCCAATACGACCAAATCTAA	93

Table S4: Primers.

Target	Company	Cat. no.	Application
IWS1	Cell Signaling	5861	WB, ChIP
phospho-IWS1 (Ser 720)	Cell Signaling	Gift	WB, IHC
Akt1	Cell Signaling	2938	WB
Akt2	Cell Signaling	2964	WB
Akt3	Cell Signaling	8018	WB
Akt (pan)	Cell Signaling	4685	WB
phosphor-Akt (Thr 308)	Cell Signaling	4056	WB
phosphor-Akt (Ser 473)	Cell Signaling	4060	WB
HA tag	Cell Signaling	3724	ChIP
myc tag	Cell Signaling	2276	WB, ChIP
tri-methyl-histone H3 (K36)	Cell Signaling	4909	ChIP
CREB	Cell Signaling	9104	WB
phospho-Ser/Thr Akt Substrate	Cell Signaling	9611	WB, IP
phospho-Ser/Thr Akt Substrate	Cell Signaling	9614	WB, IP
RNA polymerase II	Cell Signaling	2629	WB
GFP	Cell Signaling	2956	WB
FLAG tag	Cell Signaling	2368	WB
HGK (MAP4K4)	Cell Signaling	3485	WB, IP
phospho-DNAJC2/MPP11 (S47)	Cell Signaling	12397	WB
DNAJC2/MPP11 (ZRF1)	Cell Signaling	12844	WB
phospho-PRAS40 (T246)	Cell Signaling	2997	WB, IP
PRAS40	Cell Signaling	2691	WB, IP
FLAG tag (M5)	Sigma	F4042	WB
FLAG tag (M2)	Sigma	F2426	IP
tubulin	Sigma	T5168	WB
SETD2	Sigma	AV47617	WB, IP
SPT6	Abcam	ab32820	IP
REF/Aly	GeneTex	GTX26141	IP
MRG15	Aviva Systems Biology	ARP32832_T100	ChIP
HSP90	BD Transduction Laboratories	610419	WB

Table S5: Antibody list.

EXTENDED EXPERIMENTAL PROCEDURES

Cells, culture conditions, growth factors and Akt inhibitors.

Mouse lung fibroblasts were derived from a C57Bl/6 $Akt1^{fl/fl}/Akt2^{-/-}/Akt3^{-/-}$ mouse and they were immortalized spontaneously via a 3T3 type protocol, as previously described (Iliopoulos et al., 2009). Subsequently, they were transduced with myc-Akt1, myc-Akt2, myc-Akt3 or myc-Akt1/2/3) constructs in the retroviral vector pBabe-puro, pBabe-neo, pBabe-bleo, or with the empty vector. Following selection, the endogenous floxed Akt1 allele was knocked out by pMig-GFP-Cre. This gave rise to cells that express different Akt isoforms, but are otherwise identical. To generate Akt triple knockout (TKO) cells, we transduced the immortalized $Akt1^{fl/fl}/Akt2^{-/-}/Akt3^{-/-}$ cells with pMig-GFP-Cre and we selected the infected cells by FACS sorting. The TKO cells do not proliferate, but they remain fully viable for about a week. They were used therefore immediately after they had recovered from the sorting. All the lung fibroblast-derived cell lines were cultured in DMEM (Cellgro) supplemented with 10% fetal bovine serum, penicillin and streptomycin, sodium pyruvate, nonessential amino acids, and glutamine.

Human cancer cell lines were cultured under standard culture conditions, in the growth media described in the Table S2. FGF-2 (Cell Signaling, cat. no. 8910) (20ng/ml) or IGF-1 (Cell Signaling, cat. no. 8917) (20ng/ml), were used to stimulate NCI H522, NCI H1299 or T47D cells that had been serum-starved for 16 hours. Alternatively, it was used to supplement growth media containing 1% FBS. To inhibit Akt in cells growing in complete media, we exposed them to the Akt inhibitors MK2206 (MERCK) (5 μM) or AZD5363 (AstraZeneka) (5μM) for 2 hours.

Phosphoproteomics screen and data analysis

Lysates of triple Akt knockout cells and their derivatives expressing different Akt isoforms (Akt1, Akt2, Akt3 and Akt1/2/3) were digested with LysC, and the resulting peptides were affinity purified with Akt phospho substrate antibodies. Enriched phospho-peptides were digested with trypsin and analyzed by mass spectroscopy following the published “Cell Signaling Technology” protocol (Moritz et al., 2010). Three such experiments were conducted and the phosphorylation sites

detected in one or more of these experiments were combined in a single database. We then calculated the log2 of the ratio of the abundance of each phosphorylation event in Akt1, Akt2, Akt3 and Akt1/2/3, vs TKO cells. The distribution of these values around the median allowed us to calculate the robust z score for each phosphorylation event in Akt1, Akt2, Akt3 and Akt1/2/3-expressing cells. To identify phosphorylation events mediated preferentially by some Akt isoforms, we focused on those events whose z scores place them beyond the median absolute deviation value (MAD value) of 2. This analysis was carried out by Dana Farber Bioinformatics Facility.

siRNAs, shRNAs and expression constructs. Cloning and site-directed mutagenesis

Supplementary Table S3 describes the origin of the siRNAs, shRNAs and expression constructs used in this study. The IWS1, SETD2, CALPAIN1 and CABLES1 ORFs were transferred to the pENTR/D-TOPO cloning vector (Invitrogen, cat. no. 45-0218). Following this, the IWS1 ORF was recombined to pLenti CMV Puro DEST (Addgene, cat. no. 17452), while the SETD2, CALPAIN1 and CABLES1 ORFs were recombined to pLenti CMV Neo DEST (Addgene, cat. no. 17392). FGFR IIIc, cloned in the Gateway vector pDONR (GeneCopoeia), was also recombined to pLenti CMV Neo DEST. pLenti CMV Neo DEST expressing Firefly Luciferase and pLenti CMV Puro DEST expressing GFP were used as controls. To generate the shRNA-resistant variants of IWS1 and the IWS1 phosphorylation site mutant S720A/T721A, we used the QuickChange II site directed mutagenesis kit (Agilent Stratagene, cat no. 200524-5). The same mutagenesis kit was used to generate the mutants YAP1S109A, INTS3S1034A, HSPAT265A, ATRXS785A and BCL10 T52A. The primer sets we used to generate the IWS1, SETD2, CALPAIN1 and CABLES1 lentiviral constructs, and the mutant constructs described above, are listed on the Table S4.

Transfections and infections

Retroviral constructs were packaged in 293T cells by transient transfection, in combination with ecotropic (Eco-pac) or amphotropic (Ampho-pac) packaging constructs. Lentivirus constructs were also packaged in 293T cells by transient transfection, in combination with with pCMV-VSVG and pCMV-dR8.2 dvpr. Transfections were carried out using Fugene HD (Promega, cat. no. E2311).

Infections were carried out in the presence of 5 μg/ml polybrene (Sigma, cat. no. 107689). Depending on the selection marker in the vector, infected cells were sorted by FACS (GFP or RFP), or they were selected for resistance to puromycin (Gibco, cat. no. A11138) (2 μg/ml), G-418 (Cellgro, cat. no. 30-234) (400μg/ml), or bleomycin (Sigma, cat. no. B8416-15UN) (100 μg/ml). Cells infected with multiple constructs, were selected for infection with the first construct, prior to the next infection.

Transfection of lung carcinoma cell lines with siRNAs (20 nM final concentration) were carried out, using the Lipofectamine *RNAiMAX* Transfection Reagent (Invitrogen, cat. no. 13778).

Immunoprecipitation and Immunoblotting

Cells were lysed using a Triton X-100 lysis buffer (20 mM Tris (pH 7.5), 150 mM NaCl, 1 mM EDTA, 1 mM EGTA, 1% Triton X-100, 2.5 mM Sodium pyrophosphate, 1 mM β-glycerophosphate, 1 mM Na3VO4, protease inhibitor-cocktail from Roche, phosphatase inhibitor-cocktail also from Roche and 1.2 mM PMSF). Lysates were sonicated and clarified by centrifugation at 18,000 × *g* for 15 min. The clarified lysates were either electrophoresed in SDS-PAGE or they were used for immunoprecipitation. This was done by adding the primary antibody at the recommended concentration to 500 μl (1 mg of protein) of the clarified lysates and by incubating the mixture at 4°C, with gentle rocking overnight. Protein G agarose beads (Invitrogen, cat no. 15920-010) (30 μl) were subsequently added and the mixture was incubated with gentle rocking for 1 hour at 4°C. The agarose bead-bound immunoprecipitates were washed three times, 5 min each time, at 4°C with lysis buffer and they were electrophoresed (20μg protein per lane) in SDS-PAGE. Electrophoresed lysates or immunoprecipitates were transferred to polyvinylidene difluoride membranes in 25 mM Tris, 192 mM glycine. Following blocking with 5% nonfat dry milk in TBS and 0.1% Tween-20, the membranes were probed with antibodies (at the recommended dilution), followed by horseradish peroxidase-labeled secondary antibodies (1:2000), and they were developed with Pierce ECL Western Blotting Substrate (Thermo Scientific, cat. no 32106). The antibodies were used are listed in Table S5.

In vitro kinase assay

Myc-tagged Akt1 and Akt2 were immunoprecipitated with anti–Myc-conjugated agarose beads from the myc-Akt1 or myc-Akt2-expressing lung fibroblasts described above. In vitro kinase assays were performed as previously described (Ezell et al., 2012). The phosphorylation substrates were human IWS1 wt, IWS1 S720A, IWS1 T721A and IWS1 S720A/T721A, which were expressed as GST fusion proteins in the BL21 strain of *Escherichia coli*. Recombinant GSK3α/β (Cell Signaling, cat. no. 9237) was also used as a control kinase substrate. Following induction with isopropyl-β-D-thiogalactopyranoside, the GST-fusion proteins were affinity-purified using Glutathione Sepharose beads (Amersham).

Real-time RT-PCR

Total cell RNA was extracted using Trizol (Invitrogen, cat. no 15596-026). cDNA was synthesized from 1.0 μg of total RNA, using oligo-dT priming and the Retroscript reverse transcription kit (Ambion, cat no. AM1710). Gene expression was quantified by real time PCR, using the RT^2 Real-Time SYBR Green PCR master mix system (Qiagen, cat no. 330502) and an Opticon 2 DNA Monitor instrument (Biorad). mRNA levels were normalized to *GAPDH*, which was used as an internal control. The primer sets used for all the real time PCR assays throughout this report are listed on the Table S4.

Chromatin Immunoprecipitation (ChIP)

ChIP was performed using a Chromatin Immunoprecipitation assay kit (Millipore, cat no. 17-295) and following the instructions of the manufacturer. Chromatin cross-linking was achieved via a 10 minute treatment of nuclear extracts with 1% formaldehyde at 37^{o}C. Cross-linked lysates were sonicated to shear the DNA to an average length of 200 to 1000 base pairs. Following sonication, the lysates were pre-cleared via incubation with a 50% slurry of salmon sperm DNA/Protein A Agarose for 30 minutes. The pre-cleared supernatants were incubated with the primary antibody (1:50 dilution) overnight and with salmon sperm DNA/Protein A Agarose beads at 4°C for 1 h. Following multiple washes, the DNA-protein complexes were eluted and the DNA was recovered by

reverse cross-linking with NaCl and proteinase K. The DNA was then extracted using Qiaquick PCR Purification Kit (Qiagen, cat. no 28106) and it was analyzed by SYBR-Green real-time qPCR, along with the input DNA. Exon 3 of the *GAPDH* genomic locus, which is constitutively-spliced, was used as the control for chromatin IPs of the *FGFR-2* gene. The primer sets used are listed on the Table S4.

Cell proliferation, migration and invasion assays

Cell proliferation was monitored in cells growing in complete media and in cells growing in media supplemented with 1% FBS and 20 ng/ml FGF-2. Cells were seeded in 48well plates (10^4 cells / well) and the relative number of cells was measured at 24 hour intervals with the 3-(4,5-dimethylthiazol-2-yl)-2,5-diphenyltetrazolium bromide (MTT) assay (Invitrogen, cat no. M6494).

Non-directional migration was measured with the wound healing assay as previously described (Kottakis et al., 2011). Briefly, serum starved confluent cell monolayers were wounded with a plastic pipette tip and after three washes with PBS, they were cultured in serum-free RPMI supplemented with 20ng/ml FGF-2. The wounded areas were photographed 24 hours later and cell migration was measured with the Adobe Photoshop CS3 software.

Directional cell migration was measured with the transwell filter assay, using 24well microchemotaxis chambers with uncoated polycarbonate membranes (pore size 8μm) (Costar, cat no. 3422) (Kottakis et al., 2011). $5x10^4$ cells were placed in the upper chamber and they migrated toward the FGF-2-containing media, placed in the lower chamber.

In vitro invasion assays were performed using BD BioCoat Matrigel Invasion Chambers (BD Biosciences, cat no. 354480), as previously described (Hatziapostolou et al., 2011). $5x10^4$ cells were placed in the chamber and they invaded the FGF-2 (20ng/ml)-containing matrigel.

Tumor xenografts

$2x10^6$ shControl, shIWS1, shIWS1wt rescue or shIWS1mut rescue NCI H1299 cells were injected subcutaneously in the right flank of nude mice (Charles River Laboratories). Tumor growth was

monitored once a week for a total of 4 weeks. Tumor volumes were calculated with the equation $V\ (mm^3) = \frac{1}{2}ab^2$, where a is the largest diameter and b is the diameter that is perpendicular to a. Two xenograft experiments were carried out with six mice per cell type in the one and 4 mice per cell type in the other. At 4 weeks, xenografts were harvested and formalin-fixed. Paraffin embedded sections were stained with H and E or they were used for immunohistochemistry. The tumor size at each time point was presented as the mean ± SE.

Immunohistochemistry

Human lung tumor and normal tissue array (Biochain Institute Inc., cat no. T8235732) and formalin-fixed paraffin-embedded sections of the xenograft tumors were stained with the specific anti-phospho-IWS1 S720 antibody. The sections were deparafinized with xylene (3x5 min) followed by 2x10 min washes with 100% and 95% ethanol and 2x5 min washes with ddH_2O. Antigen unmasking was achieved by boiling the samples in a 10 mM sodium citrate buffer, pH 6.0 and by maintaining the samples at a sub-boiling temperature for 10 more minutes in the same buffer. Tissue sections were then washed three times with ddH_2O, incubated in 3% hydrogen peroxide for 20 minutes, washed twice with ddH_2O and once with TBS-T (TBS, 0.1% Tween-20) and blocked with 5% normal goat serum (Cell Signaling, cat no. 5425) in TBS-T for 1 hour at room temperature. Phospho-IWS1 S720 antibody was dilutied 1:50 in Signal Stain antibody diluent (Cell Signaling, cat no. 8112) and incubated with the sections overnight at 4 ^{o}C. Following this, the samples were washed x3, 5 min each, with TBS-T and incubated with an HRP-conjugated anti-rabbit IgG secondary antibody (Cell Signaling, cat no. 8114) for 30 minutes at room temperature. After 3 more 5 minute washes with TBS-T, sections were stained, using the DAB Peroxidase Substrate Kit (Vector Laboratories, cat no. SK-4100) for 20 min, washed and counterstained with hematoxylin QS (Vector Laboratories, cat no. H-3404). Stained tissues were dehydrated and mounted in Eukitt medium. Images were captured with a Nikon 80i Upright Microscope equipped with a Nikon Digital Sight DS-Fi1 color camera, using the NISElements image acquisition software.

Protein and RNA isolation from frozen tumors

Tumors were homogenized with the TissueLyser LT (Qiagen), using 5mm stainless steel beads and following the instructions of the manufacturer. For RNA isolation we used TRIzol® Reagent (Ambion, cat. no. 15596-026). For protein extraction we used RIPA buffer (BostonBioProducts, cat. no. BP-115) plus cocktail tablets of protease inhibitors (Roche, cat. no. 11697498001) and phosphatase inhibitors (Roche, cat. no. 04906845001).

Database search for SETD2 mutations

Since the recruitment of SETD2 is a critical step in the regulation of the alternative splicing pathway described in this report, we performed database searches to determine whether it may be a target of mutations in lung cancer. These searches showed that SETD2 is not mutated in the cell lines NCI H522 and NCI H1299 (http://www.broadinstitute.org/ccle/home). However, mutations in SETD2 were detected in primary human lung cancer (http://cancer.sanger.ac.uk/cosmic/gene/analysis?ln=SETD2#histo). It is not yet known whether some of these mutations may allow the recruitment of SETD2 to the IWS1 complex, in the absence of IWS1 phosphorylation.

SUPPLEMENTAL REFERENCES

Abe, Y., Yoon, S.O., Kubota, K., Mendoza, M.C., Gygi, S.P., and Blenis, J. (2009). p90 ribosomal S6 kinase and p70 ribosomal S6 kinase link phosphorylation of the eukaryotic chaperonin containing TCP-1 to growth factor, insulin, and nutrient signaling. J Biol Chem *284*, 14939-14948.

Alessi, D.R., Caudwell, F.B., Andjelkovic, M., Hemmings, B.A., and Cohen, P. (1996). Molecular basis for the substrate specificity of protein kinase B; comparison with MAPKAP kinase-1 and p70 S6 kinase. FEBS Lett *399*, 333-338.

Auld, G.C., Campbell, D.G., Morrice, N., and Cohen, P. (2005). Identification of calcium-regulated heat-stable protein of 24 kDa (CRHSP24) as a physiological substrate for PKB and RSK using KESTREL. Biochem J *389*, 775-783.

Bertrand, L., Alessi, D.R., Deprez, J., Deak, M., Viaene, E., Rider, M.H., and Hue, L. (1999). Heart 6-phosphofructo-2-kinase activation by insulin results from Ser-466 and Ser-483 phosphorylation and requires 3-phosphoinositide-dependent kinase-1, but not protein kinase B. J Biol Chem *274*, 30927-30933.

Berwick, D.C., Hers, I., Heesom, K.J., Moule, S.K., and Tavare, J.M. (2002). The identification of ATP-citrate lyase as a protein kinase B (Akt) substrate in primary adipocytes. J Biol Chem *277*, 33895-33900.

Biggs, W.H., 3rd, Meisenhelder, J., Hunter, T., Cavenee, W.K., and Arden, K.C. (1999). Protein kinase B/Akt-mediated phosphorylation promotes nuclear exclusion of the winged helix transcription factor FKHR1. Proc Natl Acad Sci U S A *96*, 7421-7426.

Boehm, J.S., Zhao, J.J., Yao, J., Kim, S.Y., Firestein, R., Dunn, I.F., Sjostrom, S.K., Garraway, L.A., Weremowicz, S., Richardson, A.L.*, et al.* (2007). Integrative genomic approaches identify IKBKE as a breast cancer oncogene. Cell *129*, 1065-1079.

Brunet, A., Bonni, A., Zigmond, M.J., Lin, M.Z., Juo, P., Hu, L.S., Anderson, M.J., Arden, K.C., Blenis, J., and Greenberg, M.E. (1999). Akt promotes cell survival by phosphorylating and inhibiting a Forkhead transcription factor. Cell *96*, 857-868.

Brunet, A., Park, J., Tran, H., Hu, L.S., Hemmings, B.A., and Greenberg, M.E. (2001). Protein kinase SGK mediates survival signals by phosphorylating the forkhead transcription factor FKHRL1 (FOXO3a). Mol Cell Biol *21*, 952-965.

Burchfield, J.G., Lennard, A.J., Narasimhan, S., Hughes, W.E., Wasinger, V.C., Corthals, G.L., Okuda, T., Kondoh, H., Biden, T.J., and Schmitz-Peiffer, C. (2004). Akt mediates insulin-stimulated phosphorylation of Ndrg2: evidence for cross-talk with protein kinase C theta. J Biol Chem *279*, 18623-18632.

Cai, S.L., Tee, A.R., Short, J.D., Bergeron, J.M., Kim, J., Shen, J., Guo, R., Johnson, C.L., Kiguchi, K., and Walker, C.L. (2006). Activity of TSC2 is inhibited by AKT-mediated phosphorylation and membrane partitioning. J Cell Biol *173*, 279-289.

Campeau, E., Ruhl, V.E., Rodier, F., Smith, C.L., Rahmberg, B.L., Fuss, J.O., Campisi, J., Yaswen, P., Cooper, P.K., and Kaufman, P.D. (2009). A versatile viral system for expression and depletion of proteins in mammalian cells. PLoS One *4*, e6529.

Cenni, V., Bertacchini, J., Beretti, F., Lattanzi, G., Bavelloni, A., Riccio, M., Ruzzene, M., Marin, O., Arrigoni, G., Parnaik, V.*, et al.* (2008). Lamin A Ser404 is a nuclear target of Akt phosphorylation in C2C12 cells. J Proteome Res *7*, 4727-4735.

Chen, S., Murphy, J., Toth, R., Campbell, D.G., Morrice, N.A., and Mackintosh, C. (2008). Complementary regulation of TBC1D1 and AS160 by growth factors, insulin and AMPK activators. Biochem J *409*, 449-459.

Chiu, T., Santiskulvong, C., and Rozengurt, E. (2005). EGF receptor transactivation mediates ANG II-stimulated mitogenesis in intestinal epithelial cells through the PI3-kinase/Akt/mTOR/p70S6K1 signaling pathway. Am J Physiol Gastrointest Liver Physiol *288*, G182-194.

Cross, D.A., Alessi, D.R., Cohen, P., Andjelkovich, M., and Hemmings, B.A. (1995). Inhibition of glycogen synthase kinase-3 by insulin mediated by protein kinase B. Nature *378*, 785-789.

Deprez, J., Vertommen, D., Alessi, D.R., Hue, L., and Rider, M.H. (1997). Phosphorylation and activation of heart 6-phosphofructo-2-kinase by protein kinase B and other protein kinases of the insulin signaling cascades. J Biol Chem *272*, 17269-17275.

Dustin, M.L., Olszowy, M.W., Holdorf, A.D., Li, J., Bromley, S., Desai, N., Widder, P., Rosenberger, F., van der Merwe, P.A., Allen, P.M.*, et al.* (1998). A novel adaptor protein orchestrates receptor patterning and cytoskeletal polarity in T-cell contacts. Cell *94*, 667-677.

Ezell, S.A., Polytarchou, C., Hatziapostolou, M., Guo, A., Sanidas, I., Bihani, T., Comb, M.J., Sourvinos, G., and Tsichlis, P.N. (2012). The protein kinase Akt1 regulates the interferon response through phosphorylation of the transcriptional repressor EMSY. Proc Natl Acad Sci U S A *109*, E613-621.

Fonseca, S.G., Fukuma, M., Lipson, K.L., Nguyen, L.X., Allen, J.R., Oka, Y., and Urano, F. (2005). WFS1 is a novel component of the unfolded protein response and maintains homeostasis of the endoplasmic reticulum in pancreatic beta-cells. J Biol Chem *280*, 39609-39615.

Guan, K.L., Figueroa, C., Brtva, T.R., Zhu, T., Taylor, J., Barber, T.D., and Vojtek, A.B. (2000). Negative regulation of the serine/threonine kinase B-Raf by Akt. J Biol Chem *275*, 27354-27359.

Hageman, J., and Kampinga, H.H. (2009). Computational analysis of the human HSPH/HSPA/DNAJ family and cloning of a human HSPH/HSPA/DNAJ expression library. Cell Stress Chaperones *14*, 1-21.

Hanaoka, K., Qian, F., Boletta, A., Bhunia, A.K., Piontek, K., Tsiokas, L., Sukhatme, V.P., Guggino, W.B., and Germino, G.G. (2000). Co-assembly of polycystin-1 and -2 produces unique cation-permeable currents. Nature *408*, 990-994.

Hatziapostolou, M., Polytarchou, C., Aggelidou, E., Drakaki, A., Poultsides, G.A., Jaeger, S.A., Ogata, H., Karin, M., Struhl, K., Hadzopoulou-Cladaras, M.*, et al.* (2011). An HNF4alpha-miRNA inflammatory feedback circuit regulates hepatocellular oncogenesis. Cell *147*, 1233-1247.

Huang, J., Gong, Z., Ghosal, G., and Chen, J. (2009). SOSS complexes participate in the maintenance of genomic stability. Mol Cell *35*, 384-393.

Huang, X., Begley, M., Morgenstern, K.A., Gu, Y., Rose, P., Zhao, H., and Zhu, X. (2003). Crystal structure of an inactive Akt2 kinase domain. Structure *11*, 21-30.

Humphrey, S.J., Yang, G., Yang, P., Fazakerley, D.J., Stockli, J., Yang, J.Y., and James, D.E. (2013). Dynamic adipocyte phosphoproteome reveals that Akt directly regulates mTORC2. Cell Metab *17*, 1009-1020.

Iliopoulos, D., Polytarchou, C., Hatziapostolou, M., Kottakis, F., Maroulakou, I.G., Struhl, K., and Tsichlis, P.N. (2009). MicroRNAs differentially regulated by Akt isoforms control EMT and stem cell renewal in cancer cells. Sci Signal *2*, ra62.

Inoki, K., Li, Y., Zhu, T., Wu, J., and Guan, K.L. (2002). TSC2 is phosphorylated and inhibited by Akt and suppresses mTOR signalling. Nat Cell Biol *4*, 648-657.

Irie, H.Y., Pearline, R.V., Grueneberg, D., Hsia, M., Ravichandran, P., Kothari, N., Natesan, S., and Brugge, J.S. (2005). Distinct roles of Akt1 and Akt2 in regulating cell migration and epithelial-mesenchymal transition. J Cell Biol *171*, 1023-1034.

Kottakis, F., Polytarchou, C., Foltopoulou, P., Sanidas, I., Kampranis, S.C., and Tsichlis, P.N. (2011). FGF-2 regulates cell proliferation, migration, and angiogenesis through an NDY1/KDM2B-miR-101-EZH2 pathway. Mol Cell *43*, 285-298.

Kovacina, K.S., Park, G.Y., Bae, S.S., Guzzetta, A.W., Schaefer, E., Birnbaum, M.J., and Roth, R.A. (2003). Identification of a proline-rich Akt substrate as a 14-3-3 binding partner. J Biol Chem *278*, 10189-10194.

Kumar, C.C., and Madison, V. (2005). AKT crystal structure and AKT-specific inhibitors. Oncogene *24*, 7493-7501.

Larance, M., Rowland, A.F., Hoehn, K.L., Humphreys, D.T., Preiss, T., Guilhaus, M., and James, D.E. (2010). Global phosphoproteomics identifies a major role for AKT and 14-3-3 in regulating EDC3. Mol Cell Proteomics *9*, 682-694.

Lee, I.H., Dinudom, A., Sanchez-Perez, A., Kumar, S., and Cook, D.I. (2007). Akt mediates the effect of insulin on epithelial sodium channels by inhibiting Nedd4-2. J Biol Chem *282*, 29866-29873.

Lee, Y.H., Campbell, H.D., and Stallcup, M.R. (2004). Developmentally essential protein flightless I is a nuclear receptor coactivator with actin binding activity. Mol Cell Biol *24*, 2103-2117.

Liao, R.G., Jung, J., Tchaicha, J., Wilkerson, M.D., Sivachenko, A., Beauchamp, E.M., Liu, Q., Pugh, T.J., Pedamallu, C.S., Hayes, D.N.*, et al.* (2013). Inhibitor-sensitive FGFR2 and FGFR3 mutations in lung squamous cell carcinoma. Cancer Res *73*, 5195-5205.

Manning, B.D., Tee, A.R., Logsdon, M.N., Blenis, J., and Cantley, L.C. (2002). Identification of the tuberous sclerosis complex-2 tumor suppressor gene product tuberin as a target of the phosphoinositide 3-kinase/akt pathway. Mol Cell *10*, 151-162.

Mayo, L.D., and Donner, D.B. (2001). A phosphatidylinositol 3-kinase/Akt pathway promotes translocation of Mdm2 from the cytoplasm to the nucleus. Proc Natl Acad Sci U S A *98*, 11598-11603.

Moritz, A., Li, Y., Guo, A., Villen, J., Wang, Y., MacNeill, J., Kornhauser, J., Sprott, K., Zhou, J., Possemato, A*., et al.* (2010). Akt-RSK-S6 kinase signaling networks activated by oncogenic receptor tyrosine kinases. Sci Signal *3*, ra64.

Mouton, V., Vertommen, D., Bertrand, L., Hue, L., and Rider, M.H. (2007). Evaluation of the role of protein kinase Czeta in insulin-induced heart 6-phosphofructo-2-kinase activation. Cell Signal *19*, 52-61.

Murray, J.T., Campbell, D.G., Peggie, M., Mora, A., and Cohen, P. (2004). Identification of filamin C as a new physiological substrate of PKBalpha using KESTREL. Biochem J *384*, 489-494.

Nave, B.T., Ouwens, M., Withers, D.J., Alessi, D.R., and Shepherd, P.R. (1999). Mammalian target of rapamycin is a direct target for protein kinase B: identification of a convergence point for opposing effects of insulin and amino-acid deficiency on protein translation. Biochem J *344 Pt 2*, 427-431.

Nelson, A.C., Lyons, T.R., Young, C.D., Hansen, K.C., Anderson, S.M., and Holt, J.T. (2010). AKT regulates BRCA1 stability in response to hormone signaling. Mol Cell Endocrinol *319*, 129-142.

Overholtzer, M., Zhang, J., Smolen, G.A., Muir, B., Li, W., Sgroi, D.C., Deng, C.X., Brugge, J.S., and Haber, D.A. (2006). Transforming properties of YAP, a candidate oncogene on the chromosome 11q22 amplicon. Proc Natl Acad Sci U S A *103*, 12405-12410.

Palamarchuk, A., Efanov, A., Maximov, V., Aqeilan, R.I., Croce, C.M., and Pekarsky, Y. (2005). Akt phosphorylates and regulates Pdcd4 tumor suppressor protein. Cancer Res *65*, 11282-11286.

Park, H.S., Kim, M.S., Huh, S.H., Park, J., Chung, J., Kang, S.S., and Choi, E.J. (2002). Akt (protein kinase B) negatively regulates SEK1 by means of protein phosphorylation. J Biol Chem *277*, 2573-2578.

Polytarchou, C., Iliopoulos, D., Hatziapostolou, M., Kottakis, F., Maroulakou, I., Struhl, K., and Tsichlis, P.N. (2011). Akt2 regulates all Akt isoforms and promotes resistance to hypoxia through induction of miR-21 upon oxygen deprivation. Cancer Res *71*, 4720-4731.

Ran, R., Pan, R., Lu, A., Xu, H., Davis, R.R., and Sharp, F.R. (2007). A novel 165-kDa Golgin protein induced by brain ischemia and phosphorylated by Akt protects against apoptosis. Mol Cell Neurosci *36*, 392-407.

Rena, G., Guo, S., Cichy, S.C., Unterman, T.G., and Cohen, P. (1999). Phosphorylation of the transcription factor forkhead family member FKHR by protein kinase B. J Biol Chem *274*, 17179-17183.

Roux, P.P., Ballif, B.A., Anjum, R., Gygi, S.P., and Blenis, J. (2004). Tumor-promoting phorbol esters and activated Ras inactivate the tuberous sclerosis tumor suppressor complex via p90 ribosomal S6 kinase. Proc Natl Acad Sci U S A *101*, 13489-13494.

Salinas, M., Wang, J., Rosa de Sagarra, M., Martin, D., Rojo, A.I., Martin-Perez, J., Ortiz de Montellano, P.R., and Cuadrado, A. (2004). Protein kinase Akt/PKB phosphorylates heme oxygenase-1 in vitro and in vivo. FEBS Lett *578*, 90-94.

Scheid, M.P., and Woodgett, J.R. (2001). PKB/AKT: functional insights from genetic models. Nat Rev Mol Cell Biol *2*, 760-768.

Somervaille, T.C., Linch, D.C., and Khwaja, A. (2001). Growth factor withdrawal from primary human erythroid progenitors induces apoptosis through a pathway involving glycogen synthase kinase-3 and Bax. Blood *98*, 1374-1381.

Song, J.J., and Lee, Y.J. (2005). Cross-talk between JIP3 and JIP1 during glucose deprivation: SEK1-JNK2 and Akt1 act as mediators. J Biol Chem *280*, 26845-26855.

Tang, J., Wu, S., Liu, H., Stratt, R., Barak, O.G., Shiekhattar, R., Picketts, D.J., and Yang, X. (2004). A novel transcription regulatory complex containing death domain-associated protein and the ATR-X syndrome protein. J Biol Chem *279*, 20369-20377.

Tominaga, K., Leung, J.K., Rookard, P., Echigo, J., Smith, J.R., and Pereira-Smith, O.M. (2003). MRGX is a novel transcriptional regulator that exhibits activation or repression of the B-myb promoter in a cell type-dependent manner. J Biol Chem *278*, 49618-49624.

Trencia, A., Perfetti, A., Cassese, A., Vigliotta, G., Miele, C., Oriente, F., Santopietro, S., Giacco, F., Condorelli, G., Formisano, P*., et al.* (2003). Protein kinase B/Akt binds and phosphorylates PED/PEA-15, stabilizing its antiapoptotic action. Mol Cell Biol *23*, 4511-4521.

van Gorp, A.G., van der Vos, K.E., Brenkman, A.B., Bremer, A., van den Broek, N., Zwartkruis, F., Hershey, J.W., Burgering, B.M., Calkhoven, C.F., and Coffer, P.J. (2009). AGC kinases regulate phosphorylation and activation of eukaryotic translation initiation factor 4B. Oncogene *28*, 95-106.

Vitari, A.C., Deak, M., Collins, B.J., Morrice, N., Prescott, A.R., Phelan, A., Humphreys, S., and Alessi, D.R. (2004). WNK1, the kinase mutated in an inherited high-blood-pressure syndrome, is a novel PKB (protein kinase B)/Akt substrate. Biochem J *378*, 257-268.

Wei, Q., and Adelstein, R.S. (2000). Conditional expression of a truncated fragment of nonmuscle myosin II-A alters cell shape but not cytokinesis in HeLa cells. Mol Biol Cell *11*, 3617-3627.

Wu, C.J., and Ashwell, J.D. (2008). NEMO recognition of ubiquitinated Bcl10 is required for T cell receptor-mediated NF-kappaB activation. Proc Natl Acad Sci U S A *105*, 3023-3028.

Wu, W.I., Voegtli, W.C., Sturgis, H.L., Dizon, F.P., Vigers, G.P., and Brandhuber, B.J. (2010). Crystal structure of human AKT1 with an allosteric inhibitor reveals a new mode of kinase inhibition. PLoS One *5*, e12913.

Xie, J., Lee, J.A., Kress, T.L., Mowry, K.L., and Black, D.L. (2003). Protein kinase A phosphorylation modulates transport of the polypyrimidine tract-binding protein. Proc Natl Acad Sci U S A *100*, 8776-8781.

Xu, B.E., Stippec, S., Lazrak, A., Huang, C.L., and Cobb, M.H. (2005). WNK1 activates SGK1 by a phosphatidylinositol 3-kinase-dependent and non-catalytic mechanism. J Biol Chem *280*, 34218-34223.

Yang, J., Cron, P., Good, V.M., Thompson, V., Hemmings, B.A., and Barford, D. (2002). Crystal structure of an activated Akt/protein kinase B ternary complex with GSK3-peptide and AMP-PNP. Nat Struct Biol *9*, 940-944.

Yang, L., Sun, M., Sun, X.M., Cheng, G.Z., Nicosia, S.V., and Cheng, J.Q. (2007). Akt attenuation of the serine protease activity of HtrA2/Omi through phosphorylation of serine 212. J Biol Chem *282*, 10981-10987.

Yoh, S.M., Cho, H., Pickle, L., Evans, R.M., and Jones, K.A. (2007). The Spt6 SH2 domain binds Ser2-P RNAPII to direct Iws1-dependent mRNA splicing and export. Genes Dev *21*, 160-174.

Yoon, S.O., Shin, S., Liu, Y., Ballif, B.A., Woo, M.S., Gygi, S.P., and Blenis, J. (2008). Ran-binding protein 3 phosphorylation links the Ras and PI3-kinase pathways to nucleocytoplasmic transport. Mol Cell *29*, 362-375.

Yoshizaki, T., Imamura, T., Babendure, J.L., Lu, J.C., Sonoda, N., and Olefsky, J.M. (2007). Myosin 5a is an insulin-stimulated Akt2 (protein kinase Bbeta) substrate modulating GLUT4 vesicle translocation. Mol Cell Biol *27*, 5172-5183.

Zhang, H., Zha, X., Tan, Y., Hornbeck, P.V., Mastrangelo, A.J., Alessi, D.R., Polakiewicz, R.D., and Comb, M.J. (2002). Phosphoprotein analysis using antibodies broadly reactive against phosphorylated motifs. J Biol Chem *277*, 39379-39387.